AN AB INITIO ANALYSIS OF STRUCTURAL, OPTICAL, ELECTRONIC, AND THERMAL PROPERTIES OF CUBIC SrSnO₃ USING WEIN2k†

Arya[a], Aditya Kumar[b], Varsha Yadav[c], Hari Pratap Bhaskar[d], Sushil Kumar[e], Satyam Kumar[e], Upendra Kumar[f,*]

[a]Department of Physics, National Institute of Science Education and Research, Jatni, Khurda-752050, Odisha, India
[b]Department of Physics, School of Science, IFTM University Moradabad-244102, U.P., India
[c]School of Applied Science, Shri Venkateshwar University, Gajraula (Amroha)-244221, U.P., India
[d]Department of Physics, Chaudhary Mahadeo Prasad Degree College Prayagraj -211002, U.P., India
[e]Department of Physics, Hansraj College, University of Delhi, New Delhi-07 India
[f]Advanced Functional Materials Laboratory, Department of Applied Sciences, IIIT Allahabad, Prayagraj-211015, U.P., India
*Corresponding author: upendrakumar@iiita.ac.in

This paper investigated the structural, optical, electronic and thermal characteristics of SrSnO₃ perovskites that were calculated using the density functional theory. Software called WEIN2K is used to perform the calculation. According to our calculations, the band gap energy of the SrSnO₃ is roughly 4.00 eV and it adopts a distorted cubic shape in the space group $Pm\bar{3}m$. The band structure and partial density of state reflects the major contribution of O 2p in the valence band while 5s orbital from Sn in the conduction band. The electron density plot significantly shows the contribution different clusters SrO₁₂ and SnO₆ that plays crucial role in electronic and optical properties. The creation of covalent bonds between the atoms of Sn and O as well as the ionic interaction between the atoms of Sr and O are both demonstrated by the electron density graphs and SCF calculation. The refractive index and extinction coefficient directly correlated with the real and imaginary part of complex dielectric function. Real part of dielectric function shows higher values at two major point of energy 3.54 eV and 9.78 eV associated with the absorption and optical activity of SrSnO₃. Negative part of imaginary dielectric function part suggests metallic behavior also supported by -grep lapw method. Thermoelectric and thermal conductivity properties suggest the power factor need to be improved for the device application.

Keywords: Density functional calculations; Electronic structure; Effective masses; Dielectric permittivity, Optical properties.
PACS: 71.15.Mb; 71.20.-b; 71.55.Ak; 72.20.Pa

The universal chemical formula for perovskite stannate oxides is ASnO₃ [1]. The alkaline earth stannate perovskites are one of the primary compounds in this group of minerals. Site A is occupied by alkaline earth metals including calcium (Ca), strontium (Sr), and barium (Ba), whose ionic radii vary from 100 pm to 135 pm [2]. In example, photovoltaic cells and light-emitting organic diodes have made extensive use of them to manufacture transparent electrodes for a variety of applications. Because of its outstanding dielectric and gas sensing qualities, ASnO₃ is very commonly utilised in electronics [3,4]. These perovskite compounds are used as anodes in Li-ion batteries and are made by destroying the crystal structure to produce sedentary metal oxides that are electrochemically active Sn metal. They are also promising materials for hydrogen synthesis and photocatalytic degradation [4,5].

The strontium stannate structure (SrSnO₃), which is the manuscript's main subject, is given special consideration. Sr²⁺ ions and 12 oxygen atoms occupy a dodecahedral site created by four [SnO₆] octahedrons to produce the crystalline structure of SrSnO₃ [6]. The Sn⁴⁺ cation is situated in the core of these octahedrons, which are made up of oxygen at their vertices. Due of the octahedral inclination that creates an orthorhombic structure (space group $Pbnm$) at ambient temperature, the unit cell of SrSnO₃ is a deformed cube [7]. Due to the extremely high mobility and concentration of carriers, SrSnO3 can also exist in other polymorphs ($Imma$, I4/mcm, and Pm3m) depending on the temperature increase [8].

In particular, SrSnO₃ is produced using a variety of synthesis techniques due to the scientific and technological interest in its applications. In order to clarify the effects of epitaxial tension on thin SrSnO₃ films, Gao et al. demonstrated that SrSnO₃ can be produced through a traditional solid-state reaction at high temperatures by combining an experimental investigation with a theoretical approach through DFT calculations using the LDA method [9]. Similar to this, a study conducted by Zhang et al. used DFT calculations implemented in the VASP simulation package, the revised Perdew-Burke-Ernzerhof function for solids (PBEsol) for structural relaxation, and Heyde-Scuseriae-Ernzerhof (HSE06) for the electronic structure analysis to explain the ferroelectricity induced by SrSnO₃ deformation and coupling, showing promising photovoltaic properties for use in solar cell devices [10].

Here, we carry out an ab-initio calculation for the strontium stannate structure (SrSnO₃) to show how the electrical properties are connected to various clusters, each of which has a distinct bonding environment based on the electron density distribution. Sr²⁺ ions are located in the corners of the cube in the crystal structure of SrSnO₃, while Sn ions are found with six oxygen atoms to form [SnO₆] octahedrons. The Sn⁴⁺ cation is situated in the core of these octahedrons, which are made up of oxygen at their vertices. SrSnO₃'s unit cell resembles a warped cube that produces an orthorhombic

structure (space group $Pm\bar{3}m$). Depending on the temperature range, additional SrSnO$_3$ structures exist as well (Imma, I4/mcm, and Pbnm). Furthermore, a structure-property relationship is established in this paper's detailed analysis of the structural characteristics in order to explain the electrical structure and the bandgap (E$_{gap}$) region.

METHODOLOGY

The full-potential linearized augmented plane waves (FPLAPW) method of the WIEN2k package is employed to examine the characteristics of SrSnO3. The exchange-correlation perspective employs the PBE sol generalised gradient approximation GGA. The modified Becke-Johnson potential proposed by Tran and Blaha (TB-mBJ) is employed for the self-consistent field (SCF) computations for the evolution of band gaps because the GGA underrates band gap values. In order to evaluate the outcomes of the predicted density functional theory (DFT). The FP-LAPW method is used to determine all energy-dependent characteristics. When spin-orbit interaction was removed, -6.0 Ry was chosen as the core cut-off energy. The cut-off vector of a plane wave is represented by K$_{max}$, and the value of RMT K$_{max}$=8 in the interstitial region. RMT is the minor muffin-tin radius. The magnitude of the most important vector in charge density is G$_{max}$= 16 Ry 1/2. Fourier expansion, and l_{max} = 10 for the angular momentum expansion. A fine k-mesh of 8×8×8 was chosen because thermoelectric and optical planning require a denser k-mesh for the convergence. When the total energy approaches 105 Ry, the iteration comes to an end. Boltzmann's transport theory, which establishes the parameters of thermoelectric transport as carried out by the BoltzTraP code, can be used to evaluate the thermoelectric transport tensors [11]. Using the interpolated band structure in WIEN2k, the BoltzTraP function produces the necessary derivatives to estimate the transport parameters. The direction of the k-vector determines the band index and relaxation duration, and this direction was kept constant in the BoltzTrap algorithm.

RESULTS

The parameters listed below can be used to discuss about the physicochemical properties of SrSnO$_3$ according to the results of the Wein2K DFT simulation software.

Energy-Volume optimization and crystal structure

The experimental results of SrSnO3 with a $Pm\bar{3}m$ space group, lattice parameters of a = b = c = 4.12 Å, and angles of $\alpha = \beta = \gamma = 90^o$. The Sr atom is located at coordinates (0,0,0), Sn at coordinates (0.5,0.5,0.5), and O at coordinates (0.5, 0.5, 0); (0, 0.5, 0.5); and (0.5, 0, 0.5). The energy-volume (E-V) optimised curve shown in Figure 1 indicates that the minimal amount of energy required by a construction is around 450 a.u^3. We determine more exact lattice parameters using the data below.

The cubic perovskite ($Pm\bar{3}m$) bulk structure of SrSnO$_3$ has been optimized, and its lattice parameters a = b = c = 4.08 Å, angles α = β = γ = 90º. The Sr atom is located at the coordinates (0,0,0), Sn atom (0.5,0.5,0.5) at the centre of cube, while the O atoms present at (0.5, 0.5, 0); (0, 0.5, 0.5) and (0.5, 0, 0.5), resulting in a model with 5 formula unit per structure (see Figure 2). Due to the well-known tendency of this function to overstate the strength of interatomic interactions, the value of lattice parameters obtained after optimization is smaller than that of the literature [12].
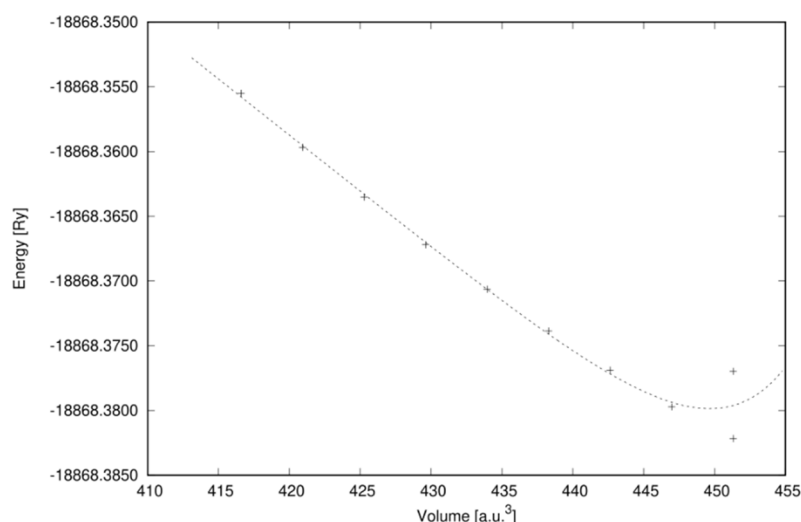

Figure 1. Energy vs. Volume curve using the volume optimization method for perovskite SrSnO$_3$
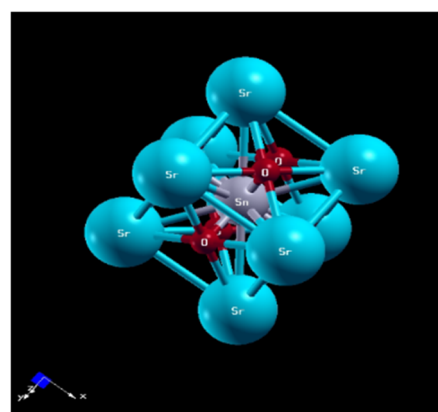

Figure 2. Crystal structure of perovskite SrSnO$_3$

Band structure and density of states (DOS)

The bonding between atoms and other desirable qualities are better understood by being familiar with the material's electrical characteristics. As illustrated in Figure 3, the band structure and density of state (DOS) projections on the

particles and atomic orbitals of strontium, tin, and oxygen were used to examine the electronic properties. The DOS figure demonstrates that the valence band and conduction band, which overlap in the plot, are primarily produced from Sn and Oxygen states. Maximum energy at which the valence band can form is 4.0 eV or less [13]. In contrast, the combination of Sr states with O upper orbitals creates the conduction band between -16.0 eV and -14.0 eV.
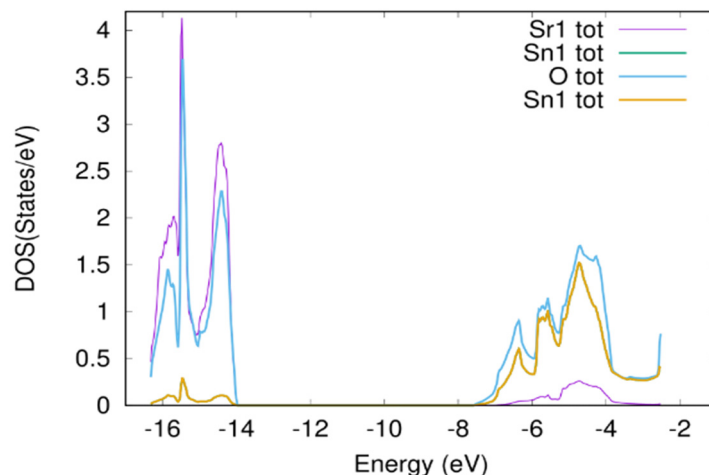

Figure 3. Total density of state (DOS) curve along with different individual atoms' DOS.

As illustrated in Figure 4, the integration of the reciprocal space for all calculations involving the SrSnO3 material used the k-points Γ (0,0,0) – X (½, 0,0) R (½, ½, ½) – M (½, ½, 0) – Γ (0,0,0). It can be observed in Figure 4 that the bandgap for SrSnO3 is an indirect transition between the k-points R-Γ with a value equal to 4.00 eV. The valence band (VB) zone is found between -17.91 and 0 eV, while the conduction band (CB) region is found between 4.18 and 29.84 eV, according to analysis of the DOS projection (Figure 4). Figure 4 shows the DOS projection for the atomic orbitals of Sr, Sn, and O atoms, showing that the three oxygen atoms have equivalent contributions and present the major contribution along with the VB through the 2s and 2p (x, y, z) orbitals combined with a minor extent of the Sr atomic orbitals 4p (x, y, z) on the other hand, the Sn atoms contribute more significantly to CB with the 5s, 5p (x, y, z), and 5d (xz, yz, and xy) orbitals [13-15].
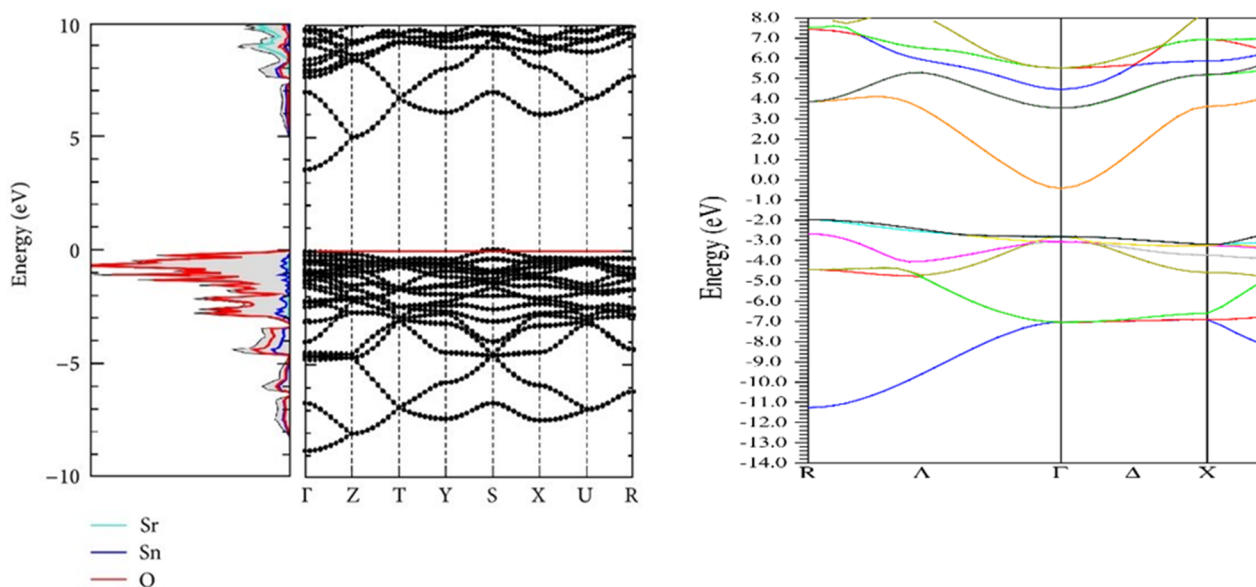

Figure 4. Band structure and partial density of state (PDOS) for cubic SrSnO₃ perovskite oxide.

Electron density around different atoms

On the basis of the charge density maps and 3D images, we further analyse the distribution of the electronic density along the crystalline structure. Isolines represent the same electrical density, which makes it easier to comprehend how chemical bonds are described. In order to identify and study the bonding interactions, the crystallographic plane is in the direction (1,1,0). The electronic density distribution of the O, Sn, and Sr atoms that make up the crystalline structure of SrSnO₃, which forms two different kinds of chemical bonds, is shown in Figure 5(a). Due to the O atom's lack of d orbitals, the pattern of electron density varies near different atoms [10,13]. While the O-Sr-O connection is demonstrated by an

ionic exchange, the O-Sn-O interaction is defined by a covalent interaction between these atoms. From the results of Figure 5(b), it feasible to observe that the isolines are shared by the nuclei on the yellow-hued Sn-O bond axes. The isolines are primarily focused on the nuclei of the Sr and O atoms, demonstrating the ionic nature of the Sr-O interactions.
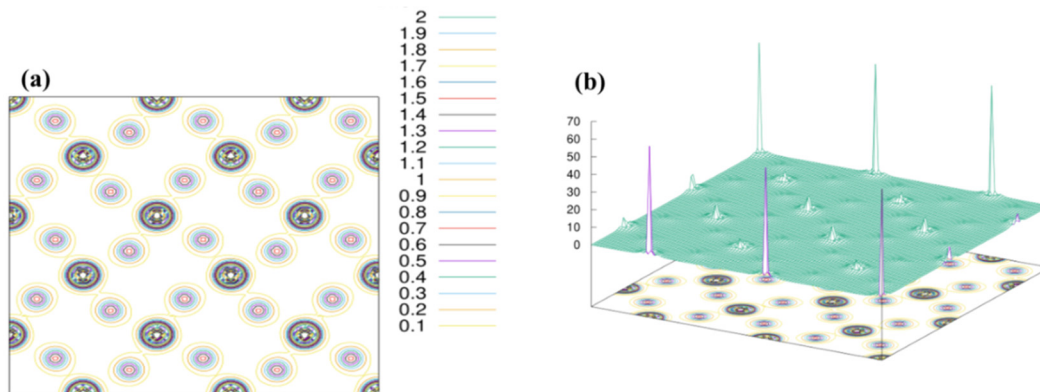

Figure 5. (a) Electron density 2D plot (b) Electron density 3D plot
(The yellow line shows the ionic interaction between oxygen and strontium).

Analysis of Total energy (ENE), Fermi energy (FER), and distribution of charge around spheres (CTO)
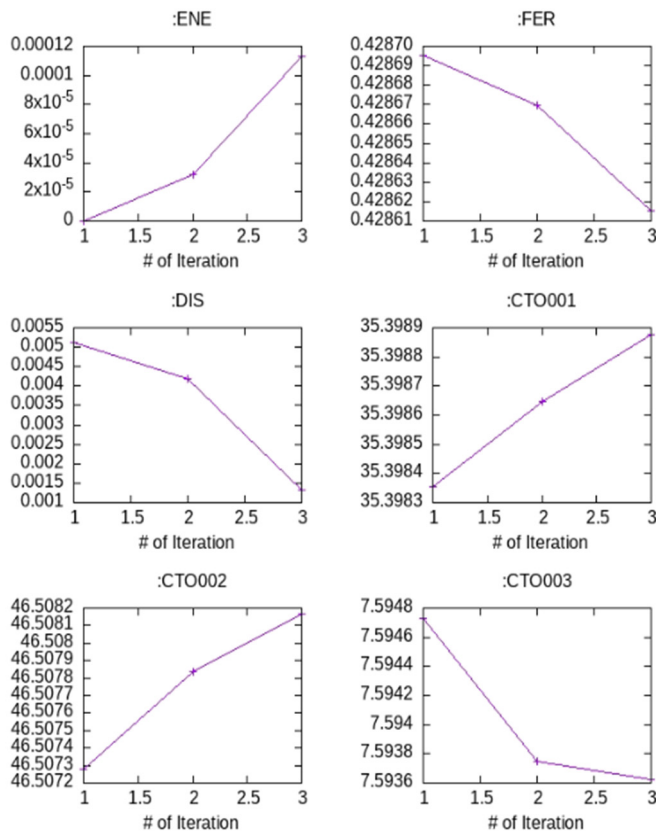

Figure 6. SCF analysis plotted vs. per number of Iteration. (ENE: total energy, FER: fermi energy, CTO01: Total charge in sphere Sr, CTO02: Total charge in sphere Sn, CTO03: Total charge in sphere O).

The overlap between these densities, which helps to produce chemical bonds in the various clusters [SrO$_{12}$] and [SnO$_6$], is another approach to examine the distribution of electrons around the nuclei. SCF cycle findings, as displayed in Figure 6, can be used to investigate the behaviour of the electronic density and crystalline structure.

The CTOXX (XX no. associated with each atom, O1-Sr, O2-Sn, O3-O) represents plots showing the total charge in a sphere at a time. In this framework, the positive slopes indicate that the overlap is adequate for forming the chemical bond, typically related to the covalent bonds. In contrast, the negative slope indicates that the orbitals' overlap occurs through a destructive interaction that disfavors the formation of the chemical bond and the resulting ionic bond. Based on the results related to charging overlap for Sr-O and Sn-O bonds of bulk SrSnO$_3$ and the charge density map, it was possible to describe the formation of covalent bonds between the Sn and O atoms with a value of 0.154 and ionic interaction between the Sr and O with a value of -0.006.

Optical properties

The optical structure of SrSnO$_3$ was measured precisely by applying the mBJ-potential technique on k-points with 4×4×4 order as we can see that the band gap is between visible and near-ultraviolet region, due to which SrSnO$_3$ is a potential candidate for solar cells and some others optoelectronic devices. The dielectric function $\varepsilon(\omega)$ is a complex function: $\varepsilon(\omega) = \varepsilon_1(\omega) + i\varepsilon_2(\omega)$, where the real part $\varepsilon_1(\omega)$ characterizes the dispersion of the incident radiation by the medium and the imaginary one $\varepsilon_2(\omega)$ describes the absorbed energy by the medium. The plot for the real part of the dielectric function $\varepsilon_1(\omega)$ and $\varepsilon_2(\omega)$ were shown in Figures 7 (a) and (b), respectively. The value of $\varepsilon_1(0)$ was intense at 3.54 eV and 9.78 eV, respectively. After that, it decreases and finally attains zero. The values of $\varepsilon_1(\omega)$ are found negative between 24 to 28 eV for SrSnO$_3$, which is not shown here. The negative values of $\varepsilon_1(\omega)$ indicate that incident light is reflected from the material surface, which exhibits the metallic behavior of a compound [13,16]. Metallic

behavior can also be checked using the -grep lapw command associated with the software. The imaginary part of the dielectric function of optical materials is a crucial parameter in designing optoelectronic devices. The maximum absorption intensity of incident light in a particular region and the energy band gap can be measured using $\varepsilon_2(\omega)$ for the target material. The critical value of $\varepsilon_2(\omega)$ is between 4.15-6.0eV. The refractive index n(ω) and extinction coefficient k(ω) can also be calculated with the help of the following equation; $n_2 - k_2 = \varepsilon_1$ and $2n_1k_1 = \varepsilon_2$, where subscript 1 represents the real part and 2 represents the imaginary part of the refractive index and extinction coefficient, respectively. From the graphical analysis, the n(ω) and k(ω) will follow a similar trend as $\varepsilon_1(\omega)$, $\varepsilon_2(\omega)$. The relation between the static value of n(0) and $\varepsilon_1(0)$ is $2 = \varepsilon_1(0)$, which satisfies the result. Furthermore, n(ω) is a dimensionless quantity that describes energy propagation in a material. The value of n(ω) varies with a wavelength of light because of dispersion, due to which light splits into its constituent colors. The higher value of the refractive index is significant in the optical field, and the materials have in the range of one and two. In our case, the maximum value of n(ω) may be found between 7-9 eV for $SrSnO_3$ due to the higher value observed for ε_1 in this range. The middle peaks of the graph are analyzed, which disappear at higher energy, implying that at higher energy, the transparency of materials decreases, and high energy photons are absorbed due to band transition from valance to conduction.
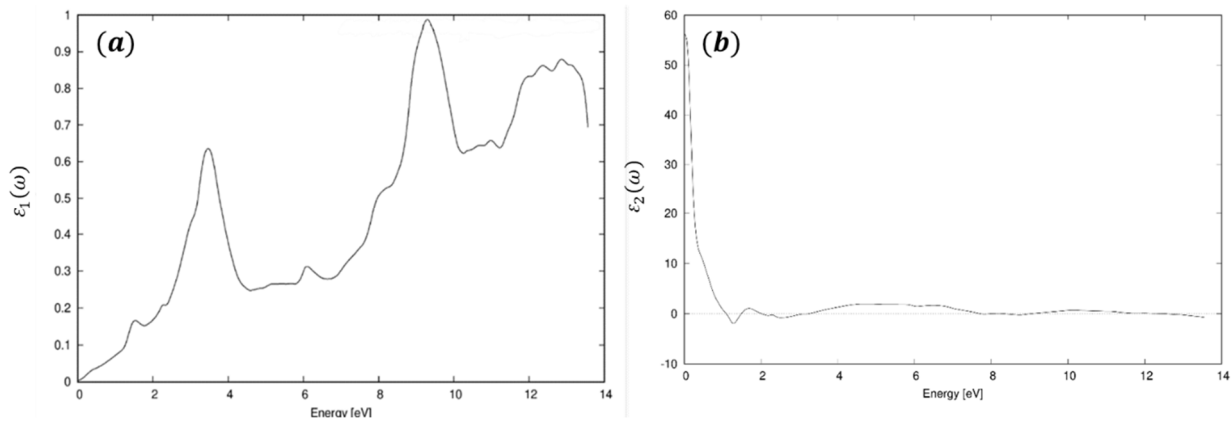

Figure 7. (a) $\varepsilon_1(\omega)$ (b) $\varepsilon_2(\omega)$ as a function of energy for cubic $SrSnO_3$

Thermoelectric properties

Thermoelectric materials have attracted huge consideration recently due to their applications ranging from clean energy to photon sensing devices. These materials are used in solid-state Peltier coolers and in generating waste heat. The variations in the essential transport properties like the Seebeck coefficient (S), electrical, thermal conductivity (k), electrical conductivity (σ), and power factor that could be represented as σS^2 as a function of temperature are valuable to explain the thermoelectric enactment of $SrSnO_3$. The power factor needs to be increased to improve the thermoelectric behavior that necessitates greater values of S and σ [16]. In contrast, the representation of electrical and thermal conductivity is essential, as shown in Figures 8(a) and (b).
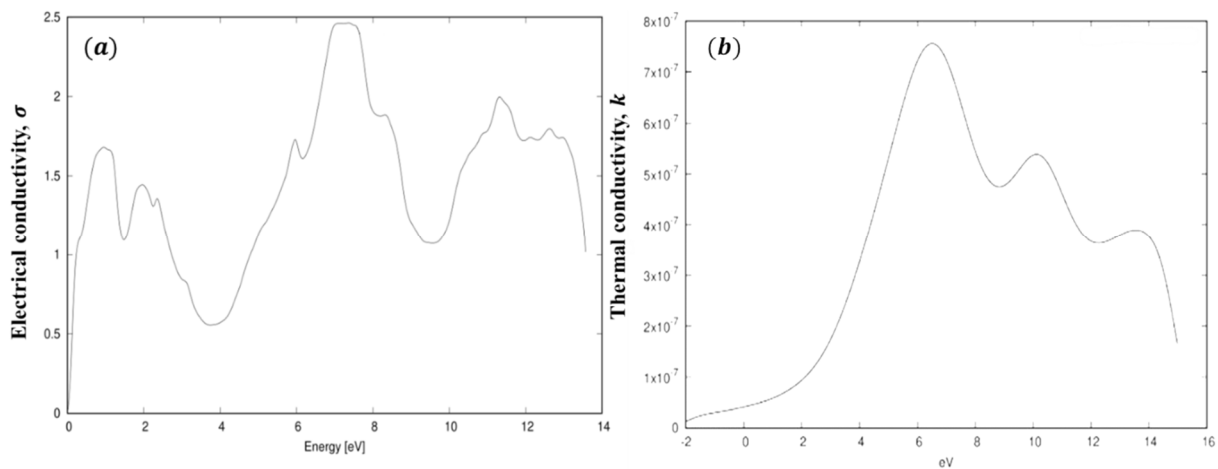

Figure 8. (a) Electrical conductivity, (b) Thermal conductivity, as a function of energy for cubic $SrSnO_3$.

The efficiency of the energy conversion devices for harvesting waste heat and converting it into usable electrical energy is overseen by a dimensionless parameter that is called a figure of merit (ZT), defined as $ZT = S^2\sigma T/k_e$, where S is the Seebeck coefficient (thermopower), σ is the electrical conductivity, T is the absolute temperature, and k_e is the thermal conductivity associated with an electron of the material, respectively [14]. The electrical conductivity increases strongly with

increasing charge carrier concentration. However, the thermal conductivity is noticeably anisotropic. The power factor can be calculated from the present values of electrical conductivity and thermal conductivity with the Seebeck coefficient reported in the literature for SrSnO$_3$; PF= S$^2\sigma$ and the figure of merit can be calculated by the formula ZT=σTS$^2/k_e$ [12]. We find that SrSnO$_3$ can attain an efficiency of 0.07, expanding the calculated electrical and thermal conductivity values.

CONCLUSION

The analysis of SrSnO3 based on DFT theory provides us with a perspective to understand, interpret, and analyze the structural and electronic properties of the compound at the atomic level. The lattice parameter, bond structure, and other parameters on some level agree with the other work done on the same material. It was possible to observe that, in general, the valence band is occupied by electronic states originating from O and Sr atoms, while Sn atoms occupy the conduction band. The band gap was calculated as 4.00 eV, an indirect electron transfer process. Moreover, the SCF analysis confirms the covalent and ionic bond interaction. Therefore, the theoretical results using the Wein2K, B3LYP functional combined with the basis set for Sr, Sn, and O provided promising results in calculating structural and electronic properties. Data also provided insight that SrSnO3 can be an excellent alternative material for future transparent conductive devices.

ORCID IDs
Arya, https://orcid.org/0000-0002-8444-7461; **Aditya Kumar**, https://orcid.org/0000-0003-2823-774X
Varsha Yadav, https://orcid.org/0000-0003-1990-5910; **Hari Prasad Bhaskar**, https://orcid.org/0000-0002-1890-8936
Sushil Kumar, https://orcid.org/0000-0001-7415-9450; **Satyam Kumar**, https://orcid.org/0000-0001-7101-9559
Upendra Kumar, https://orcid.org/0000-0001-9200-0048

REFERENCES
[1] M. Glerup, K.S. Knight, and F.W. Poulsen, "High temperature structural phase transitions in SrSnO$_3$ perovskite", Mater. Res. Bull. **40**, 507 (2005). https://doi.org/10.1016/j.materresbull.2004.11.004

[2] R.D. Shannon, "Revised effective ionic radii and systematic studies of interatomic distances in halides and chalcogenides", Acta Crystallogr. Sect. A. **32**, 751 (1976). https://doi.org/10.1107/S0567739476001551

[3] A. Vegas, M. Vallet-Regí, J.M. González-Calbet, and M.A. Alario-Franco, "The ASnO3 (A=Ca,Sr) perovskites", Acta Crystallogr. Sect. B. **42**, 167 (1986). https://doi.org/10.1107/S0108768186098403

[4] Y. Liu, Y. Zhou, D. Jia, J. Zhao, B. Wang, Y. Cui, Q. Li, and B. Liu, "Composition dependent intrinsic defect structures in ASnO3 (A = Ca, Sr, Ba)", J. Mater. Sci. Technol. **42**, 212 (2020). https://doi.org/10.1016/j.jmst.2019.10.015

[5] Y.A. Zulueta, R. Mut, S. Kaya, J.A. Dawson, and M.T. Nguyen, "Strontium Stannate as an Alternative Anode Material for Li-Ion Batteries", J. Phys. Chem. C. **125**, 14947 (2021). https://doi.org/10.1021/acs.jpcc.1c02652

[6] A. Kumar, B. Khan, V. Yadav, A. Dixit, U. Kumar, and M.K. Singh, "Rietveld refinement, optical, dielectric and ac conductivity studies of Ba-doped SrSnO$_3$", J. Mater. Sci. Mater. Electron. **31**, 16838 (2020). https://doi.org/10.1007/s10854-020-04240-7

[7] E. Cortés-Adasme, R. Castillo, S. Conejeros, M. Vega, and J. Llanos, "Behavior of Eu ions in SrSnO$_3$: Optical properties, XPS experiments and DFT calculations", J. Alloys Compd. **771**, 162 (2019). https://doi.org/10.1016/j.jallcom.2018.08.239

[8] A.L. Goodwin, S.A.T. Redfern, M.T. Dove, D.A. Keen, and M.G. Tucker, "Ferroelectric nanoscale domains and the 905 K phase transition in SrSnO$_3$: A neutron total-scattering study", Phys. Rev. B, **76**, 174114 (2007). https://doi.org/10.1103/PhysRevB.76.174114

[9] Q. Gao, K. Li, L. Zhao, K. Zhang, H. Li, J. Zhang, and Q. Liu, "Wide-range band-gap tuning and high electrical conductivity in La-and Pb-doped SrSnO$_3$ epitaxial films", ACS Appl. Mater. Interfaces, **11**, 25605 (2019). https://doi.org/10.1021/acsami.9b07819

[10] M.M. de Moura Bezerra, M.C. Oliveira, W.D. Mesquita, A.B. da Silva Junior, E. Longo, and M.F. do Carmo Gurgel, "An Ab Initio Analysis of Structural and Electronic Properties of Cubic SrSnO$_3$", Orbital Electron. J. Chem. 227 (2021). http://dx.doi.org/10.17807/orbital.v13i3.1603

[11] A.A. Adewale, A. Chik, R.M. Zaki, F.C. Pa, Y.C. Keat, and N.H. Jamil, "Thermoelectric transport properties of SrTiO$_3$ doped with Pm", Solid State Phenom. Trans. Tech. Publ, **280**, 3 (2018). https://doi.org/10.4028/www.scientific.net/SSP.280.3

[12] L. Salik, A. Bouhemadou, K. Boudiaf, F.S. Saoud, S. Bin-Omran, R. Khenata, Y. Al-Douri, and A.H. Reshak, "Structural, elastic, electronic, magnetic, optical, and thermoelectric properties of the diamond-like quaternary semiconductor CuMn$_2$InSe$_4$", J. Supercond. Nov. Magn. **33**, 1091 (2020). https://doi.org/10.1007/s10948-019-05331-1

[13] E. Moreira, J.M. Henriques, D.L. Azevedo, E.W.S. Caetano, V.N. Freire, and E.L. Albuquerque, "Structural, optoelectronic, infrared and Raman spectra of orthorhombic SrSnO$_3$ from DFT calculations", J. Solid State Chem. **184**, 921 (2011). https://doi.org/10.1016/j.jssc.2011.02.009

[14] V.V. Bannikov, I.R. Shein, V.L. Kozhevnikov, and A.L. Ivanovskii, "Magnetism without magnetic ions in non-magnetic perovskites SrTiO$_3$, SrZrO$_3$ and SrSnO$_3$", J. Magn. Magn. Mater. **320**, 936 (2008). https://doi.org/10.1016/j.jmmm.2007.09.012

[15] S. Li-Wei, D. Yi-Feng, Y. Xian-Qing, and Q. Li-Xia, "Structural, electronic and elastic properties of cubic perovskites SrSnO$_3$ and SrZrO$_3$ under hydrostatic pressure effect", Chinese Phys. Lett. **27**, 96201 (2010). https://doi.org/10.1088/0256-307X/27/9/096201

[16] H. Shaili, E. Mehdi Salmani, M. Beraich, R. Essajai, W. Battal, M. Ouafi, A. Elhat, et al, "Enhanced properties of the chemically prepared Gd-doped SrSnO$_3$ thin films: experimental and DFT study", Opt. Mater. (Amst). **107**, 110136 (2020). https://doi.org/10.1016/j.optmat.2020.110136

АВ INITIO АНАЛІЗ СТРУКТУРНИХ, ОПТИЧНИХ, ЕЛЕКТРОННИХ, ТА ТЕРМІЧНИХ ВЛАСТИВОСТЕЙ КУБІЧНОГО SrSnO₃ ЗА ДОПОМОГОЮ WEIN2k

Арья[a], Адіт'я Кумар[b], Варша Ядав[c], Харі Пратап Бхаскар[d], Сушіл Кумар[e], Сатьям Кумар[e], Упендра Кумар[f]

[a]*Фізичний факультет, Національний інститут наукової освіти та досліджень, Джатні, Кхурда-752050, Одіша, Індія*
[b]*Фізичний факультет, Наукова школа, Університет IFTM, Морадабад-244102, U.P. Індія*
[c]*Школа прикладних наук, Університет Шрі Венкатешвар, Гаджраула (Амроха)-244221, UK, Індія*
[d]*Фізичний факультет, Чаудхарі Махадео Прасад коледж, Праяградж -211002, U.P. Індія*
[e]*Фізичний факультет коледжу Хансрадж Делійського університету, Нью-Делі-07, Індія*
[f]*Лабораторія передових функціональних матеріалів, Департамент прикладних наук, IIT Аллахабад, Праяградж-211015, U.P. Індія*

У цій статті досліджено структурні, оптичні, електронні та термічні характеристики перовскітів SrSnO₃, які були розраховані за допомогою теорії густини функціоналу. Для виконання обчислень використовується програмне забезпечення під назвою WEIN2K. Відповідно до наших розрахунків, енергія забороненої зони SrSnO₃ становить приблизно 4,00 еВ, і він приймає викривлену кубічну форму в просторовій групі $Pm\overline{3}m$. Зонна структура та часткова щільність станів відображають основний внесок O 2p у валентну зону, а 5s-орбіталь від Sn у зоні провідності. Графік електронної густини суттєво показує внесок різних кластерів SrO₁₂ і SnO₆, який відіграє вирішальну роль в електронних і оптичних властивостях. Створення ковалентних зв'язків між атомами Sn і O, а також іонна взаємодія між атомами Sr і O демонструються графіками електронної густини та розрахунком SCF. Показник заломлення та коефіцієнт екстинкції прямо корелюють з дійсною та уявною частинами складної діелектричної функції. Реальна частина діелектричної функції показує вищі значення в двох основних точках енергії 3,54 еВ і 9,78 еВ, пов'язаних з поглинанням і оптичною активністю SrSnO₃. Від'ємна частина частини уявної діелектричної функції свідчить про поведінку металу, що також підтримується методом -grep lapw. Властивості термоелектричної та теплопровідності свідчать про необхідність покращення коефіцієнта потужності для застосування пристрою.

Ключові слова: розрахунки густини функціоналу; електронна структура; ефективні маси; діелектрична проникність, оптичні властивості.